A VIRTUAL ENVIRONMENT FOR ROTORCRAFT VIBRATION ANALYSIS

Aykut Tamer *, Vincenzo Muscarello[‡], Pierangelo Masarati [§], Giuseppe Quaranta [†]

Department of Aerospace Science and Technology,
Politecnico di Milano, Milano - Italy

*aykut.tamer@polimi.it [†]vincenzo.muscarello@polimi.it, [‡]pierangelo.masarati@polimi.it [§]giuseppe.quaranta@polimi.it

Abstract

This work aims at showing how a modern state space aeroservoelastic virtual simulation environment can be effective in evaluating the combined performance of several passive and active systems for helicopter vibration reduction. A general purpose helicopter model is used to demonstrate the approach. On the airframe, performance indicators are formulated based on the accelerations on the pilot seats and critical structural connection points. To illustrate the method: three helicopter-related passive vibration absorbers, which are located at main rotor hub, gearbox-fuselage connection and pilot seat, are considered.

1 INTRODUCTION

Vibrations in helicopters may limit several important factors like comfort, safety, reliability, and maximum practically attainable speed. Oscillations can also degrade handling qualities[1;2] and might even lead to chronic pain in the long-term[3]. Additionally, an excessive vibratory level leads to an increase in maintenance time, which in turn increases the operational costs. Severe vibrations may even cause structural failures and instability. Therefore, the rotorcraft should be designed to achieve the lowest possible vibrational levels[4], which in turn leads to improved acceptance for commercial market[5]. Detailed definitions, analysis, and rotorcraft applications of vibration reduction techniques can be found in Refs. 6 and 7.

In general, the vibration suppression techniques can be classified as active or passive. The passive techniques do not require any actuation and aim at isolating the critical components from high levels of vibration. Such devices may be dedicated to broadband vibration reduction, or can be optimized or dedicated to tonal vibration attenuation, when specifically tuned for a prescribed frequency. Although broadband passive attenuation devices are usually only marginally effective, the case of tonal attenuation is very interesting for helicopter applications, which are often characterized by a predominant source of vibration, the main rotor, acting at fixed frequency (N_b/rev, N_b being the number of blades). A classical method used in rotorcraft benefits from mechanical amplification of a beater mass amplified by a lever. One example is the DAVI (Dynamic Anti-resonant Vibration Isolator), which can be mounted in parallel to the gearbox suspension.[8;9]. A device that is similar in the operating concept is the ARIS (Anti-Resonance Isolation System). There are versions that can generate mechanical or hydraulic anti-resonant forces[10]. An alternative design, with the beater located in series with the gearbox suspension, is the SARIB (suspension with a resonator secured on the rod)[11], which also has a self-tuning version[12]. A different technique is to accelerate a low viscosity fluid between two chambers and let the pressure differential caused by the relative motion counteract the vibratory load[13;14;15]. The fluidlastic[1] solution is an applicative example of this concept[16]. In the rotating frame, pendulum absorbers attached on blades[17] and rotor-head vibration absorbers[18] are two proven examples.

On the other hand, active techniques are implemented through on-board computers and servo actuators, and consumes power[19]. The goal is to generate counteracting forces to reduce the oscillatory loads. Active vibration control at the rotor, i.e. at the source, is very common. An example is Higher Harmonic Control (HHC); in which the swashplate is excited at higher harmonics and the corresponding motion is superimposed to 1/rev input resulting from the cyclic commands. Application of the same system to each blade pitch link is referred to as Individual Blade Control (IBC).[20;21;22]. Active isolation is also implemented by replacing the conventional strut with a hydraulic actuator.

Semi-active techniques are also implemented as a compromise between passive and active solutions. In this case, the device is adapted to change in excitation frequency by adjusting the passive mechanical properties; for example by changing the arm length of a beater using a linear actuator. However, the semi-active and passive devices can only store or dissipate energy, thus both have the exactly same working principle[23].

[1] Fluidlastic is a trademark of Lord Corporation, Inc.

2 METHOD

Designing a vibration absorber for a helicopter is a demanding task. First of all, many critical locations on the airframe suffer from vibrations, such as pilot and passenger seats, avionics compartments, and load carrying elements. Thus, the selection of the objective of the vibration attenuation is itself a complex task. Second, since an elastic airframe possesses multiple load paths, many means of vibration suppression may be simultaneously applied on the vehicle. Third, passive vibration absorbers attenuate vibrations at the design frequency and at a prescribed location. However, at some other frequency or spatial location, they can perform in a not-optimal way; in some cases, they can even amplify vibrations, since indeed they introduce additional, very lightly damped degrees of freedom. Therefore, being a multi-objective design problem with tight constraints over a wide range of frequencies, passive vibration reduction requires a large deal of experimental work, that could be reduced significantly through the adoption of appropriate high-fidelity modeling.

The design of vibration absorbers often requires the development of several devices and a large number of iterations for parameter tuning. So, the cost associated with the analysis of a detailed model of the entire vehicle, including the absorption devices, is often not affordable. For this reason, an effective design method could take advantage of a platform for high-fidelity aeroservoelastic modeling for rotorcraft. This study proposes such a method of performance evaluation of vibration absorbers on rotorcraft.

2.1 Aeroservoelastic Rotorcraft Model

Rotorcraft aeroservoelasticity is modeled using MASST (Modern Aeroservoelastic State Space Tools), a tool developed at Politecnico di Milano. MASST analyzes compact, yet complete modular models of linearized aeroservoelastic systems[24;25]. Models are not directly formulated in MASST; they are rather composed of subcomponents collected from well-known, reliable and possibly state-of-the-art sources, which are blended together in a mathematical environment. The problem is formulated in state-space form. This approach is often termed “modern” in the automatic control community. The equations of motion of the system are cast as first-order time differential equations. Each component is modeled in its most natural and appropriate modeling environment and then cast into state-space form. Mechanical components are connected using the Craig-Bampton Component Mode Synthesis (CMS) approach[26].

Within MASST, a (virtual) sensor can be defined at any node of the rotorcraft finite element model. Then, the vibrations at the sensor locations can be found using the state space form of the MASST model. An example virtual helicopter model is given in Fig. 1. Sensors and forces can be defined at any node of the overall model.

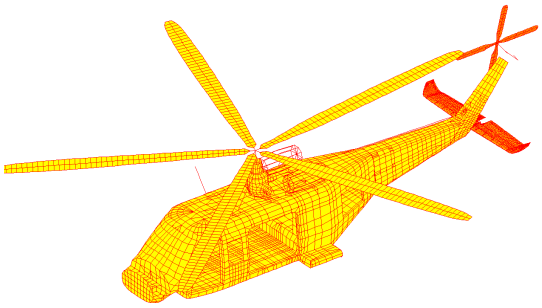

Figure 1: MASST virtual helicopter example.

Models can be highly parametric. MASST interpolates the state-space model in a generic configuration within corresponding linear models evaluated in the space of parameters that are considered.

2.2 Vibration Device Addition

In the reference configuration, the problem is represented as a linear system in state-space form:

$$\dot{\mathbf{x}} = \mathbf{A}\mathbf{x} + \mathbf{B}\mathbf{f} \tag{1a}$$

$$\mathbf{y} = \mathbf{C}\mathbf{x} + \mathbf{D}\mathbf{f} \tag{1b}$$

where vector $\mathbf{x}$ contains the states of the system, which should include the coordinates of the base model and those of the points at which the absorber is attached to. Vector $\mathbf{y}$ contains the output of the system, which, in analogy, should include both the response of the locations of the performance indicators (for example accelerations at the pilot seat) and the response of the vibration absorber device attachment positions. The inputs are the forces and moments $\mathbf{f}$ defined at some selected nodes of the model. The transfer functions for the base model and vibration absorber is formed as

$$\mathbf{y} = \mathbf{G}\mathbf{f} = \left(\mathbf{C}(\mathrm{j}\omega\mathbf{I} - \mathbf{A})^{-1}\mathbf{B} + \mathbf{D}\right)\mathbf{f} \tag{2}$$

Both active and passive vibration reduction devices can be modeled in MASST. However, within the scope of this work only passive absorbers are considered, without excessive loss of generality. For this purpose, it is necessary to define specific input and output signals in the virtual helicopter model to create the feedback path with the device. According with Fig 2:

- The input of the virtual helicopter is defined as the external forces $\mathbf{f}$ (or moments) placed on any airframe point and/or on the rotors (in this case in multiblade coordinates).
- The output $\mathbf{y}$ of the virtual helicopter model is chosen as the sensors of position, velocity, and acceleration of any airframe point (or rotor point in multiblade coordinates).
- The passive vibration absorber model creates a feedback loop between the sensors corresponding to

the motion of the points the device is attached to, and forces exerted by the absorber at its attachment points,

$$\mathbf{f}_\mathsf{A} = \mathbf{K}\mathbf{y} \tag{3}$$

such that $\mathbf{f} = \mathbf{f}_\mathsf{H} - \mathbf{f}_\mathsf{A}$, where the transfer matrix $\mathbf{K}$ represents the synthesis of the device's state-space representation

$$\dot{\mathbf{x}}_\mathsf{d} = \mathbf{A}_\mathsf{d}\mathbf{x}_\mathsf{d} + \mathbf{B}_\mathsf{d}\mathbf{y} \tag{4a}$$

$$\mathbf{f}_\mathsf{A} = \mathbf{C}_\mathsf{d}\mathbf{x}_\mathsf{d} + \mathbf{D}_\mathsf{d}\mathbf{y} \tag{4b}$$

in which vector $\mathbf{x}_\mathsf{d}$ contains the (possibly hidden) internal state of the device.

Notice that a similar scheme also applies to active vibration control devices; in that case, however, the sensors and the control forces need not be physically co-located.

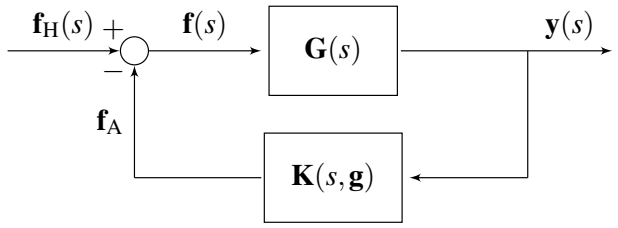

Figure 2: Block diagram representation of the vehicle ($\mathbf{G}$) and passive absorber ($\mathbf{K}$); for $s = \mathrm{j}\omega$ and $\mathbf{g}$ being tuning parameter vector.

Then the response of the modified system is obtained as:

$$\mathbf{y} = (\mathbf{I} + \mathbf{G}\mathbf{K})^{-1}\,\mathbf{G}\mathbf{f}_\mathsf{H} \tag{5}$$

Since $\mathbf{G}$ is an output of a high fidelity tool with arbitrary number of states, inputs and outputs, the gain matrix $\mathbf{K}$ can easily be defined using force-response relations of the attached device. For example, in case of a mass-spring system, it is enough to add the mass and stiffness matrices of the device to the matrix $\mathbf{K}$, considering the proper input-output channels.

2.3 Performance Indicator

For vibration reduction purposes, the objective is the reduction of the dynamic response at selected points of the rotorcraft. A scalar objective function J is written using a weighted square norm of the response vector $\mathbf{y}$. A corresponding norm of the tuning parameters vector $\mathbf{g}$, which can include mass and length for example, can contribute to the cost function. The objective function is:

$$J = \mathbf{y}^H\mathbf{W}\mathbf{y} + \mathbf{g}^H\mathbf{R}\mathbf{g} \tag{6}$$

where $\mathbf{y}^H$ and $\mathbf{g}^H$ are complex conjugate transposes (Hermitian); $\mathbf{W}$ and $\mathbf{R}$ are weighting matrices for sensor outputs and tuning parameters.

Matrix $\mathbf{W}$ defines the priority of sensor locations and of directions at each location. The elements of $\mathbf{W}$, usually but not necessarily diagonal, and positive (semi-)definite, have different values depending of their importance. Similarly, matrix $\mathbf{R}$ defines the cost of the design variables. The elements of matrices $\mathbf{W}$ and $\mathbf{R}$ must have proper units, to give correctly define the non-dimensional function J. Then, a performance indicator in percent scale can be defined using the reference value of the objective function:

$$\mathrm{PI} = \left(\frac{\mathbf{y}^T\mathbf{W}\mathbf{y} + \mathbf{g}^T\mathbf{R}\mathbf{g}}{\mathbf{y}_0^T\mathbf{W}\mathbf{y}_0} - 1 \right) \times 100\% \tag{7}$$

where the reference output is $\mathbf{y}_0 = \mathbf{G}\mathbf{f}_\mathsf{H}$.

Eq. 7 provides a frequency domain representation of a vibration performance function referred to structural points of the airframe, typically points on the cabin floor.

It should be noted that frequency-domain cabin floor accelerations may not suffice as vibration indicators when comfort or health of human pilots/passengers is considered. The whole body vibration evaluation of humans includes different aspects, subjected to frequency weighting and time averaging[27]. There exist standards for whole body vibration assessment, including but not limited to ISO-2631-1, Intrusion Index and NASA Ride Quality Model[28]. Recent application of such standards to rotorcraft-related vibration problems include the evaluation of seat cushion designs for flight engineer seats[29] and the analysis of neck strain for different flight and pilot helmet configurations[30]. Such comfort and health formulations are quite important; however, they are not considered within this work, since it focuses on vibrational level computation.

In brief, regardless of whether floor acceleration magnitude or a more involved vibration comfort assessment is required, the success of vibration performance computation depends on:

- subcomponents formulated within their most natural modeling and analysis environment;
- high-fidelity overall virtual modeling through subcomponent assembly;
- capability of defining load paths (sensor-force) between arbitrary structural points;
- exporting proper output models compatible for mounting vibration reduction solutions and calculating the performance of the resulting solutions, without the need to reassemble the whole model.

3 NUMERICAL EXAMPLES

This section illustrates the application of the tool. The first example considers the isolation of the fuselage from the gearbox using axial spring mass resonators. Each resonator is attached in parallel with the corresponding gearbox strut. The second example shows the isolation of the

pilot seat from the floor using a classic Dynamic Antiresonant Vibration Isolator (DAVI). The third example is a Mast Vibration Absorber (MVA), which is attached on the rotor head to attenuate in-plane vibrations. Finally, the simultaneous application of axial absorbers on struts and MVA on the rotor head is illustrated.

The corresponding devices are sketched in Fig. 3 at their operation locations.

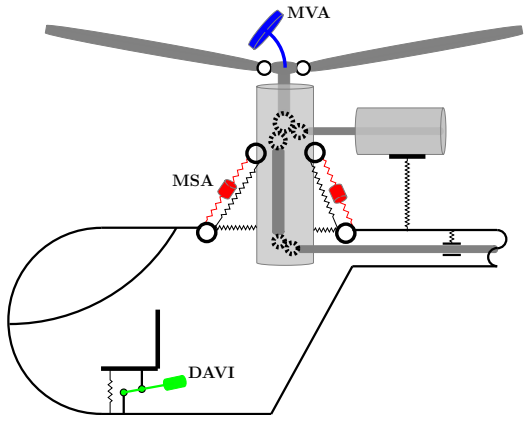

Figure 3: Representation of the illustrative vibration reduction devices: axial Mass-Spring Absorber (**MSA**) mounted parallel to the struts; a Mast Vibration Absorber (**MVA**), connected to the rotorhead via an elastic link; a Dynamic Anti-resonant Vibration Isolator (**DAVI**), connected between the pilot seat and the cabin floor

The analyses are made using a generic, medium weight 5 blade helicopter. The state-space model includes:

- Rigid body dynamics degrees of freedom;
- flight mechanics stability and control derivatives of the fuselage obtained in CAMRAD/JA;
- elastic bending and torsion modes of the airframe extracted from NASTRAN;
- first two bending modes of the main and tail rotors in multiblade coordinates obtained using CAMRAD/JA;
- main and tail rotor servo actuators formulated in Matlab/Simulink;
- the nodes and coordinates for the sensors and the forces are defined in MASST.

Although the virtual helicopter model is sufficient for vibration estimates, it should be noted that verification of the model through flight or ground test were not performed. Thus, deviations from the real behavior could exist. Moreover, the following applications are selected only for illustrative purposes, rather than as the actual means of vibration reduction of a particular rotorcraft.

3.1 Fuselage-Gearbox Isolation

The simplest form of vibration attenuation device is a Mass-Spring Absorber (MSA). Its possible application on rotorcraft can be to support a beater with two springs, which are attached to the two terminals of the struts. As given in Fig. 4, such an application aims at isolating the fuselage from the main rotor source of vibration, by properly choosing the beater mass m_b and spring stiffness k_b.

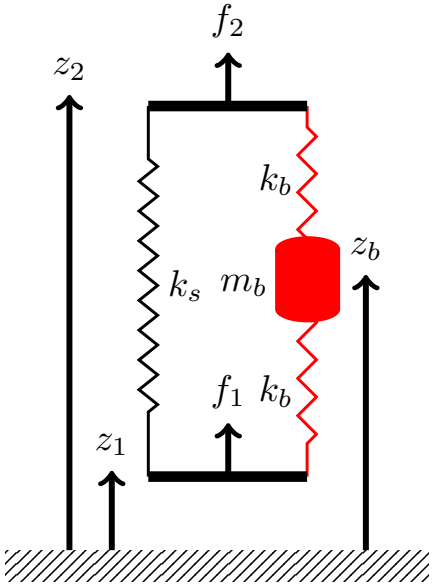

Figure 4: Axial mass-spring resonator mounted parallel to the strut.

For the purpose of isolating the fuselage from gearbox, the sensors (z_1 and z_2) and forces (f_1 and f_2) should be defined in MASST at the two ends of the strut, arbitrarily labeled as 1 and 2. The dynamics of the device can be proficiently written referring only to the local model of Fig. 4. The equation of motion of the beater is

$$k_b(z_1 - z_b) - k_b(z_b - z_2) = m_b \ddot{z}_b \tag{8}$$

where z_b is the absolute position of the beater along the device's axis. For harmonic motion, the displacement of the beater is

$$z_b = \frac{k}{2k - \omega^2 m_b}(z_1 + z_2) \tag{9}$$

The forces acting on the terminals 1 and 2 are

$$\begin{aligned} F_1 &= -k_b(z_1 - z_b) \\ &= -\left(k_b - \frac{k_b^2}{2k_b - \omega^2 m_b}\right) z_1 + \left(\frac{k_b^2}{2k_b - \omega^2 m_b}\right) z_2 \end{aligned} \tag{10}$$

$$\begin{aligned} F_2 &= k_b(z_b - z_2) = \\ &= -\left(k_b - \frac{k_b^2}{2k_b - \omega^2 m_b}\right) z_2 + \left(\frac{k_b^2}{2k_b - \omega^2 m_b}\right) z_1 \end{aligned} \tag{11}$$

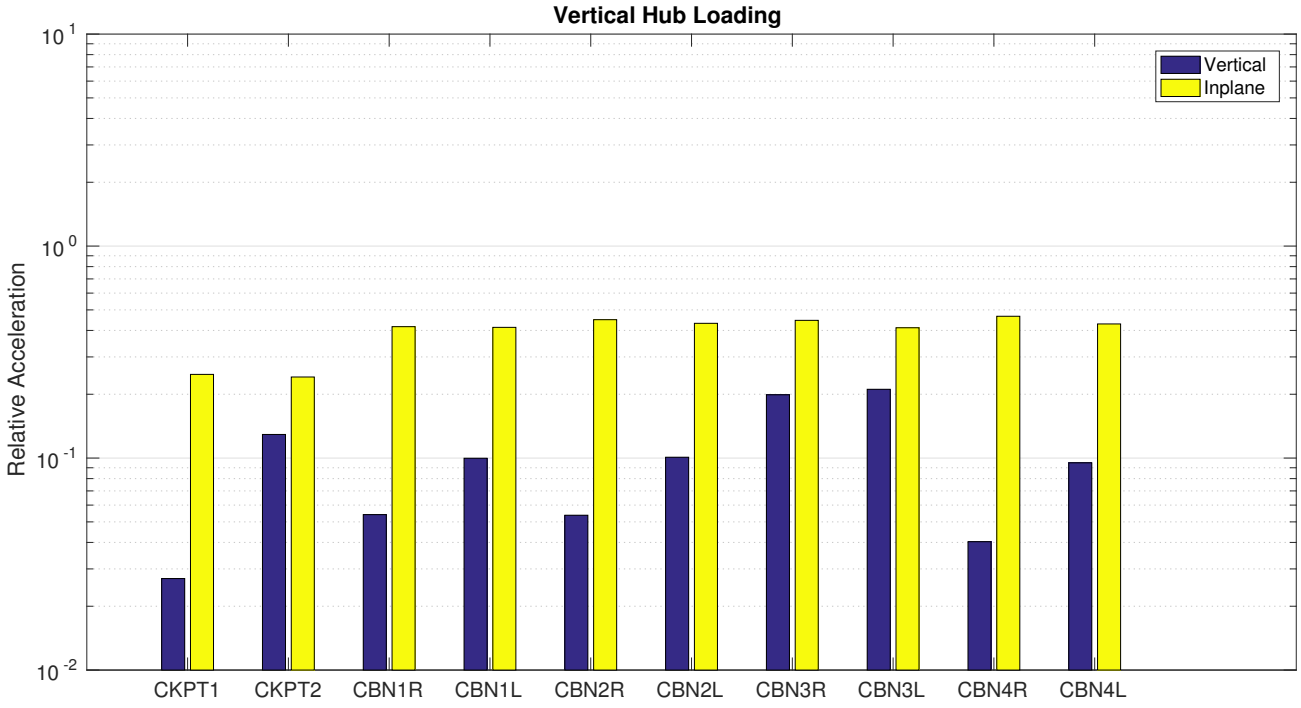

Figure 5: MSA on struts: N_b/rev acceleration of two cockpit and eight cabin sensors due to vertical hub force, relative to the nominal plant.

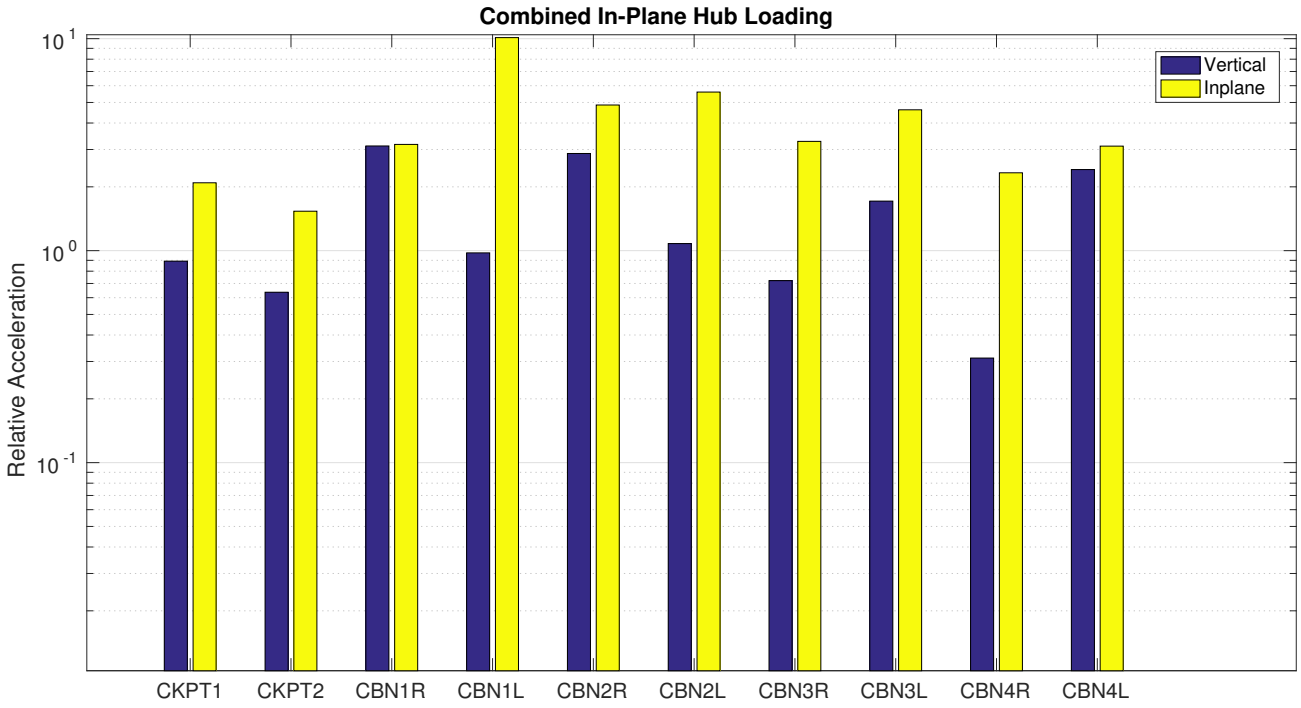

Figure 6: MSA on struts: N_b/rev acceleration of two cockpit and eight cabin sensors due to combined in-plane hub force, relative to the nominal plant.

which can be converted into the negative feedback gain matrix of Fig. 2 as:

$$(12)\qquad \begin{bmatrix} F_1 \\ \\ F_2 \end{bmatrix} = k_b \begin{bmatrix} 1-\dfrac{1}{2-\dfrac{\omega^2 m_b}{k_b}} & -\dfrac{1}{2-\dfrac{\omega^2 m_b}{k_b}} \\ -\dfrac{1}{2-\dfrac{\omega^2 m_b}{k_b}} & 1-\dfrac{1}{2-\dfrac{\omega^2 m_b}{k_b}} \end{bmatrix} \begin{bmatrix} z_1 \\ \\ z_2 \end{bmatrix}$$

Note that the strut stiffness is already included in the nominal model; therefore, it is sufficient that only the contribution of the absorber is formulated.

If the strut stiffness k_s is included in the nominal model and not exactly known a priori, the tuning values of m_b and k_b can be searched numerically. In case the stiffness of the struts is explicitly known, the tuning frequency for the isolation of terminal 2 is

$$(13)\qquad \omega = \sqrt{\left(2+\frac{k_b}{k_s}\right)\frac{k_b}{m_b}}$$

which, in case of relatively soft absorber springs, can be approximated as

$$(14)\qquad \omega \approx \sqrt{\frac{2k_b}{m_b}} \text{ for } \frac{k_b}{k_s} \ll 1$$

This represents a realistic starting value for the numerical tuning of the device.

For a 5 kg beater, the springs are tuned and the system is analyzed for vibrations at two cockpit and eight cabin locations. The excitation forces act on the main rotor hub at N_b/rev. Results are compared with the corresponding values at the same points that are obteined with the nominal nominal plant, without vibration absorption devices. Fig. 5 presents the acceleration of those points for vertical loading alone. It can be seen that at all the considered points the vertical and in-plane comfort can be improved, with better scores in the vertical direction. The same analysis is repeated for the combined in-plane loading alone, whose results are shown in Fig. 6. It can be observed that, due to the inclined geometry of the struts, the combined in-plane loads can amplify in-plane vibrations at all sensors, and increase vertical vibrations at four cabin locations.

3.2 Pilot-Seat Isolation

The DAVI, an acronym for Dynamic Antiresonant Vibration Isolator, is a mechanism that makes use of the motion of a beater mass, which is amplified using a rigid link. The rigid link is attached to two points with offset e: one side is the source of the vibration and the other is the isolation side. The amplified motion of the beater applies a counter-acting force to the vibratory force.

Attenuating the vibrations on the helicopter pilot seat using DAVI is possible[7]. The DAVI is mounted in parallel with the support of the seat, as sketched in Fig. 7.

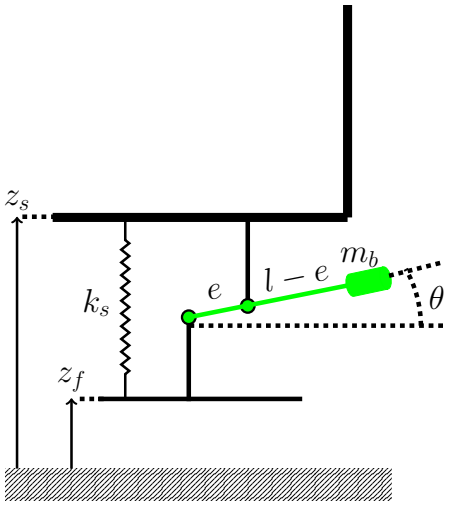

Figure 7: DAVI device under pilot seat.

The angular motion of the beater θ is a function of the difference in the displacement of the two ends:

$$(15)\qquad \theta = \frac{z_s - z_f}{e}$$

where z_s is the displacement of the seat and z_f is the displacement of the floor. The moment equilibrium about the hinge attached to the floor yields

$$(16)\qquad F_s = \frac{ml^2}{e}\ddot{\theta} = \frac{ml^2}{e^2}\left(\ddot{z}_s - \ddot{z}_f\right)$$

Similarly, the moment about the hinge attached to the seat gives:

$$(17)\qquad F_f = -\frac{ml(l-e)}{e}\ddot{\theta} = -\frac{ml(l-e)}{e^2}\left(\ddot{z}_s - \ddot{z}_f\right)$$

Writing in matrix form for a negative feedback gives the $\mathbf{K}$ matrix:

$$(18)\qquad \begin{bmatrix} F_s \\ \\ F_f \end{bmatrix} = m\frac{l^2}{e^2}\begin{bmatrix} 1 & -1 \\ \dfrac{e}{l}-1 & -\left(\dfrac{e}{l}-1\right) \end{bmatrix}\begin{bmatrix} z_s \\ \\ z_f \end{bmatrix}$$

When a spring in parallel is present, the tuning frequency ω is

$$(19)\qquad \omega = \sqrt{\frac{k_s}{m_b\lambda(\lambda-1)}}$$

where k_s is the stiffness of the seat support, m_b is the beater mass and $\lambda = l/e$ is the ratio of the distances of the beater and upper body connections to the pivot.

3.2.1 Human Vibration Model

The proposed analysis illustrates the acceleration of the seat, modeled as a rigid body connected to the cabin floor by a spring of stiffness k_s. The analysis fidelity can be further increased by adding a human vibration model, that represents the accelerations of selected body parts when excited by the motion of the seat. That of Wan and Schimmels[31] is a classical model of human body vibration, often used in comfort evaluation of road vehicles. The model

has four degrees of freedom. The human body's dynamics along the vertical axis are modeled using lumped masses, springs, and dampers. As illustrated in Fig. 8, it comprises:

- input from the seat, z_s;
- motion z_1 of body 1 with mass m_1, which is representative of the abdomen;
- motion z_2 of body 2 with mass m_2, which is representative of the bowels;
- motion z_3 of body 3 with mass m_3, which is representative of the chest;
- motion z_4 of body 4 with mass m_4, which is representative of the abdomen;
- the connections between the bodies are idealized using springs and dampers.

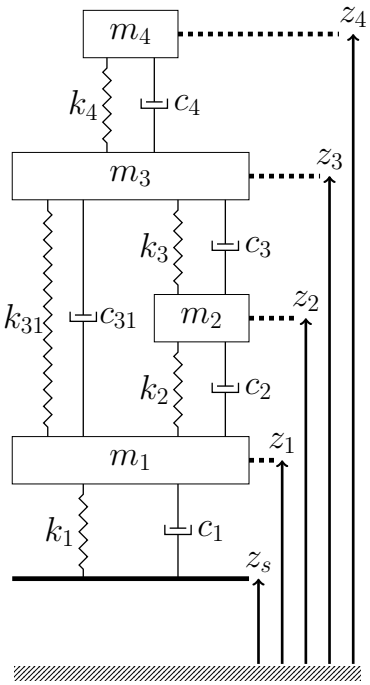

Figure 8: Wan-Schimmels lumped pilot model. Adapted from Ref.[31]

Table 1: Numerical values for the Wan-Schimmels Model[31].

	m_i (kg)	c_i ($\mathrm{N s m^{-1}}$)	k_i ($\mathrm{N m^{-1}}$)
i=1	36.00	2475.00	49341.60
i=2	5.50	330.00	20000.00
i=3	15.00	909.09	192000.00
i=4	4.17	200.00	10000.00
i=31	-	250.00	134400.00

Table 1 presents the values given in the original paper[31], which are also used in this work. The corresponding equation of motion is

$$\mathbf{M}\ddot{\mathbf{z}}_p + \mathbf{C}\dot{\mathbf{z}}_p + \mathbf{K}\mathbf{z}_p = \mathbf{f}_b \tag{20}$$

with

$$\mathbf{M} = \begin{bmatrix} m_1 & 0 & 0 & 0 \\ 0 & m_2 & 0 & 0 \\ 0 & 0 & m_3 & 0 \\ 0 & 0 & 0 & m_4 \end{bmatrix}$$

$$\mathbf{C} = \begin{bmatrix} c_1+c_2+c_{31} & -c_2 & -c_{31} & 0 \\ -c_2 & c_2+c_3 & -c_3 & 0 \\ -c_{31} & -c_3 & c_{31}+c_3+c_4 & -c_4 \\ 0 & 0 & -c_4 & c_4 \end{bmatrix}$$

$$\mathbf{K} = \begin{bmatrix} k_1+k_2+k_{31} & -k_2 & -k_{31} & 0 \\ -k_2 & k_2+k_3 & -k_3 & 0 \\ -k_{31} & -k_3 & k_{31}+k_3+k_4 & -k_4 \\ 0 & 0 & -k_4 & k_4 \end{bmatrix}$$

$$\mathbf{f}_b = \begin{bmatrix} k_1 z_0 + c_1 \dot{z}_0 & 0 & 0 & 0 \end{bmatrix}^T$$

$$\mathbf{z}_p = \begin{bmatrix} z_1 & z_2 & z_3 & z_4 \end{bmatrix}^T$$

It is worth noticing that since the total mass of the body is not negligible, its modeling within the dynamic model of the vehicle may be necessary, as using it to merely post-process the cabin floor acceleration might produce incorrect results.

The application of a DAVI under the pilot seat is examined using the numerical values given in Table 1. The results are compared with the corresponding accelerations at the floor location where seat is attached. For the body parts represented in Fig. 8, nominal and attenuated (i.e. with the DAVI device in place) cases are compared.

Fig. 9 presents the motion of the pilot head with respect to the seat floor. The dynamics of the pilot in the nominal case can amplify, see the resonance below N_b/rev, or attenuate the vibration, which reduces below that of the floor in the vicinity of and above N_b/rev. For the attenuated case with DAVI, exact anti-resonance cancellation can be achieved at N_b/rev, and the acceleration at the head is significanly reduced over the entire spectrum shown in the figure, compared with the nominal case. Similar results can be observed in Figs. 10, 11 and 12 for chest, bowels and abdomen respectively. For all cases, while no resonance exists in the vicinity of N_b/rev, anti-resonance is achieved at N_b/rev.

It is worth observing that in most cases, with the notable exception of the head, the accelerations of the body parts are attenuated with respect to those of the corresponding cabin floor location. This suggests that on the one hand the use of cabin floor accelerations may be considered conservative, whereas on the other hand it may provide excessive and misleading vibration level indications. It is posited here that the study of perceived vs. actual vibratory levels may and should take into consideration the vibratory level that the parts of the human body are subjected to.

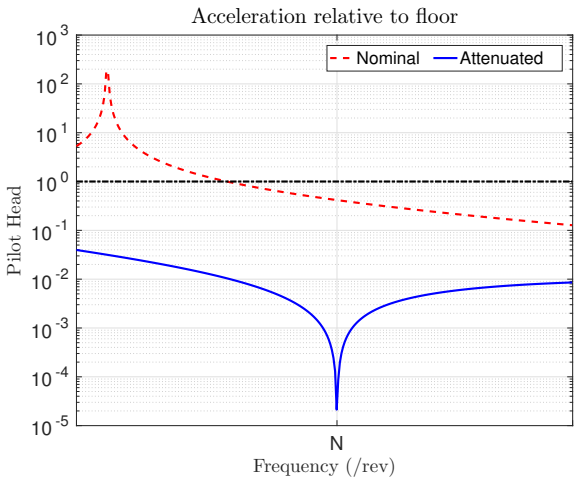

Figure 9: DAVI on seat: Acceleration of pilot head, normalized by the acceleration of the floor

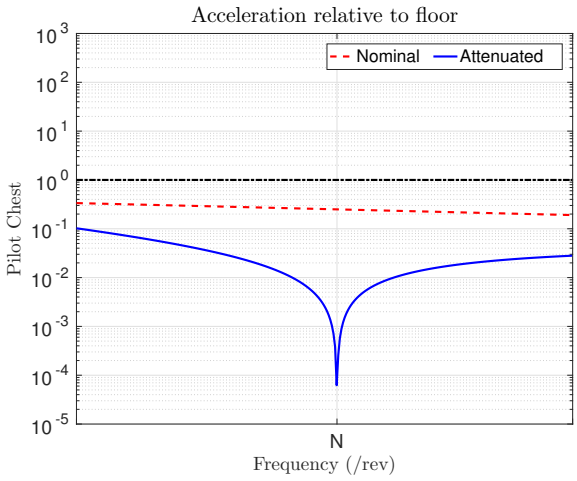

Figure 10: DAVI on seat: Acceleration of pilot chest, normalized by the acceleration of the floor

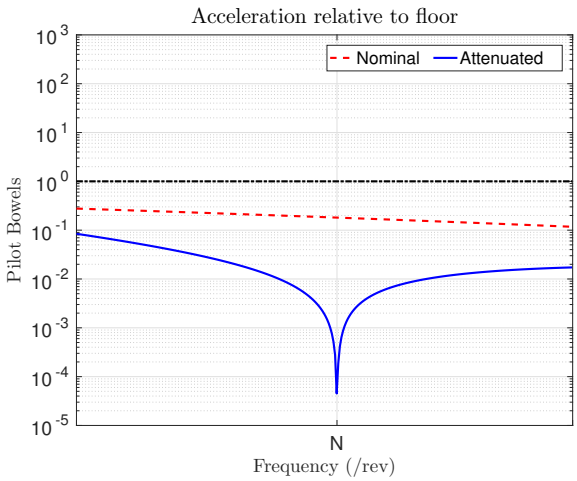

Figure 11: DAVI on seat: Acceleration of pilot bowels, normalized by the acceleration of the floor

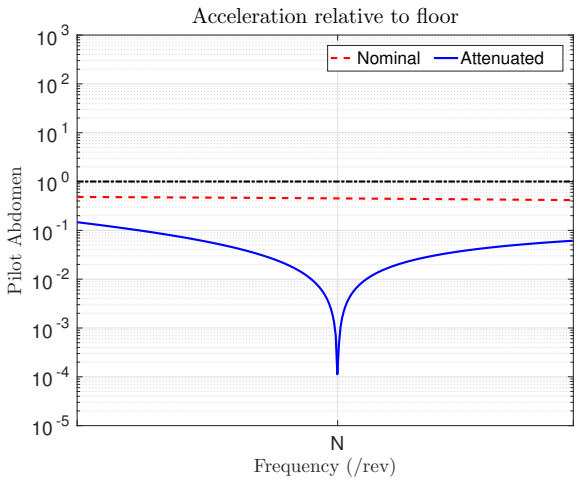

Figure 12: DAVI on seat: Acceleration of pilot abdomen, normalized by the acceleration of the floor

3.3 Mast Vibration Absorber

Mast vibration absorber (MVA) aims at reducing in-plane vibrations transmitted by the rotor mast to the gearbox and airframe. A mass is mounted on the rotor head via an elastic beam, as already sketched in Fig. 3. Since it is attached to the mast, the mass and the beam rotate with the rotor angular velocity. Fig. 13 presents an idealized and simplified MVA. The hub has mass M_h in the non-rotating frame, attached to the gearbox by springs of stiffness K_x and K_y. The MVA mass (m_a) rotates with the mast ($\psi = \Omega t$). The flexural stiffness of the beam is modeled as springs of stiffness k_x and k_y.

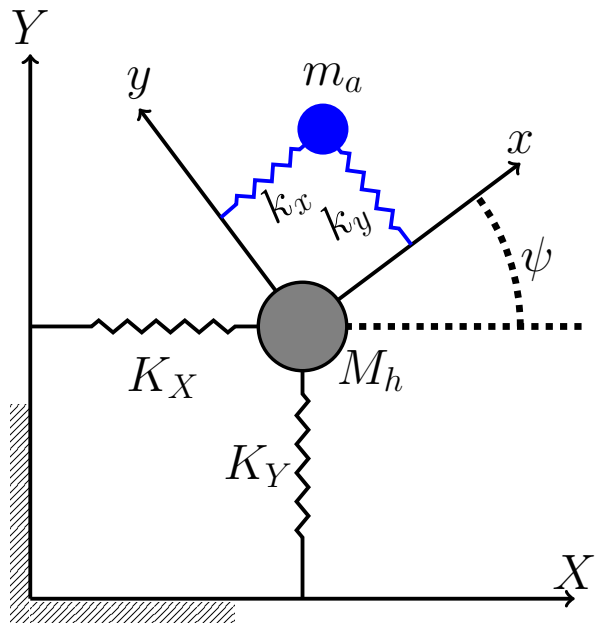

Figure 13: MVA: idealized working principle[6]

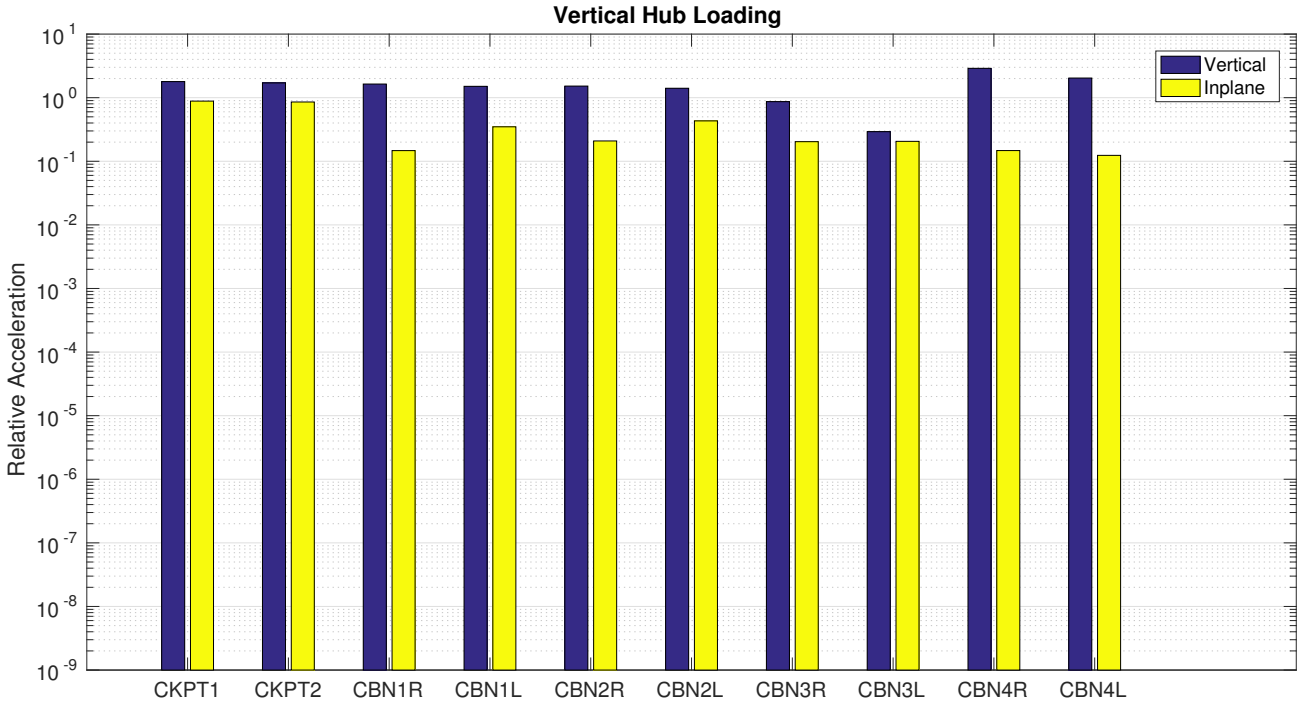

Figure 14: MVA: N_b/rev acceleration of two cockpit and eight cabin sensors due to vertical hub force, relative to the nominal plant in log scale.

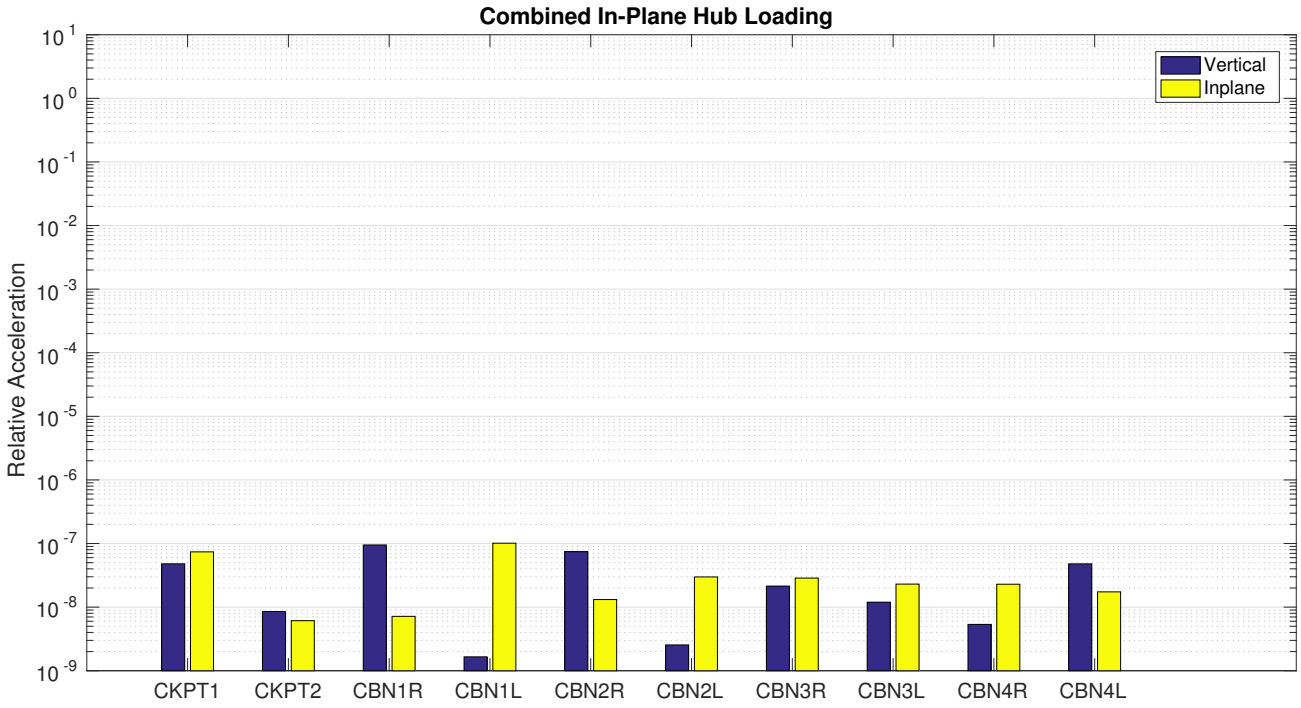

Figure 15: MVA: N_b/rev acceleration of two cockpit and eight cabin sensors due to combined in-plane hub force, relative to the nominal plant in log scale.

The equations of the idealized model are

(21)

$$\begin{bmatrix} m & 0 & m & 0 \\ 0 & m & 0 & m \\ m & 0 & m+M_r & 0 \\ 0 & m & 0 & m+M_r \end{bmatrix} \begin{bmatrix} \ddot{x} \\ \ddot{y} \\ \ddot{X} \\ \ddot{Y} \end{bmatrix} + \begin{bmatrix} k_x c^2 + k_y s^2 & (k_x - k_y)cs & 0 & 0 \\ (k_x - k_y)cs & k_x c^2 + k_y s^2 & 0 & 0 \\ 0 & 0 & K_X & 0 \\ 0 & 0 & 0 & K_Y \end{bmatrix} \begin{bmatrix} x \\ y \\ X \\ Y \end{bmatrix} = \begin{bmatrix} F_x \\ F_y \\ F_X \\ F_Y \end{bmatrix}$$

where:

c, s	$\cos\psi$, $\sin\psi$
ψ	azimuth angle of rotor
x, y	rotating reference plane of MVA
X, Y	inertial reference plane of hub
k_x, k_y	spring constants of MVA
K_X, K_Y	spring constants of hub
m	mass of MVA
M_h	mass of hub

Eq. 3.3 is a periodic function due to the terms $\sin\psi$ and $\cos\psi$, which act on the tuning springs of MVA. It can be observed that in the case of equal MVA spring constants, $k_x = k_y$, the stiffness matrix becomes time-independent and diagonal.

The $\mathbf{M}$ and $\mathbf{K}$ matrices of Eq. (3.3) are used to define the feedback loop gain matrix, considering appropriate input-output channels, keeping in mind that the hub and its connections usually are already modeled in detail in the nominal model. As such, the parameters related to the hub can be eliminated: K_y, K_y, and M_h can be set to zero.

A MVA mass of $20\,\mathrm{kg}$ is assumed, with identical MVA stiffness values, $k_x = k_y$. Fig. 14 presents the vertical and in-plane vibrations at two cockpit and eight cabin sensors as a result of only vertical hub loading. While some of the sensors show a slight increase in vibratory level, the vertical accelerations do not change on average. However, the in-plane acceleration resulting from vertical hub forces reduce at all sensor locations except CKPT1, which remains the same. Similarly, Fig. 15 presents the vertical and in-plane accelerations at the same sensors as a consequence of combined in-plane loading only. As expected considering the nature and very purpose of a MVA, the in-plane vibratory forces are attenuated quite effectively.

3.4 Simultaneous Application of Two Absorbers

The power of a modular high-fidelity vibration analysis tool is the capability to simultaneously simulate independent solutions. For example, the axial mass-spring absorbers (MSA) of Section 3.1 can effectively attenuate the vibrations originating from the vertical hub forces, while they can amplify vibrations caused by in-plane hub loads. On the other hand, the mast vibration absorber (MVA) of Section 3.3 can be quite effective in reducing the vibrations resulting from in-plane hub forces, but is essentially ineffective when the vertical hub force is the vibration source. Such results suggest that the simultaneous application of both devices might have an overall beneficial effect with respect to all components of accelerations resulting from all components of hub loads.

The previous examples show that a vibration reduction environment should be able to consider the simultaneous applications of different options, which is also beneficial for optimizing the response at a reduced cost of additional masses. To illustrate the simultaneous evaluation of two absorbers, axial MSA devices parallel to struts and a MVA on the rotor head are applied together. The same mass and spring values of the applications in Section 3.1 and 3.3 are considered.

The results are presented in Fig. 16 for the vertical hub force and in Fig. 17 for the combined in-plane loading. As expected, all component of the vibrations at the two cockpit and eight cabin sensors can be effectively reduced.

4 CONCLUSIONS

A virtual environment for helicopter vibration analysis and an effective tool for incorporating arbitrary vibration reduction devices is presented. The method is illustrated using three vibration reduction solutions: axial mass-spring absorbers parallel to the main gearbox suspension struts; a mast vibration absorber (MVA) mounted on the rotor head, and a dynamic anti-resonant vibration absorber (DAVI) mounted under the pilot seat.

In brief:

- MASST, developed at Politecnico Di Milano, is a high-fidelity state-space aeroservoelastic environment;
- MASST assembles sub-components modeled in their most natural modeling and analysis environments using Craig-Bampton approach. Frequently used sub-components include but are not limited to: rotors in multi-blade coordinates, fuselage, sensors, forces, actuators and flight mechanics stability derivatives;
- MASST enables a vibration engineer to receive high-fidelity nominal plant state-space matrices and work on the vibration attenuation solutions without spoiling the nominal model;
- the vibration reduction solutions are added as sort of feedback controllers. It is sufficient that the related input-output channels are previously defined in the nominal model;
- sensors and external forces can be defined at any position prescribed on the nominal model, allowing a detailed formulation of the vibration reduction objective function;
- an arbitrary number of vibration reduction solutions can be evaluated simultaneously, thus allowing the overall effect and defining an accurate cost function.

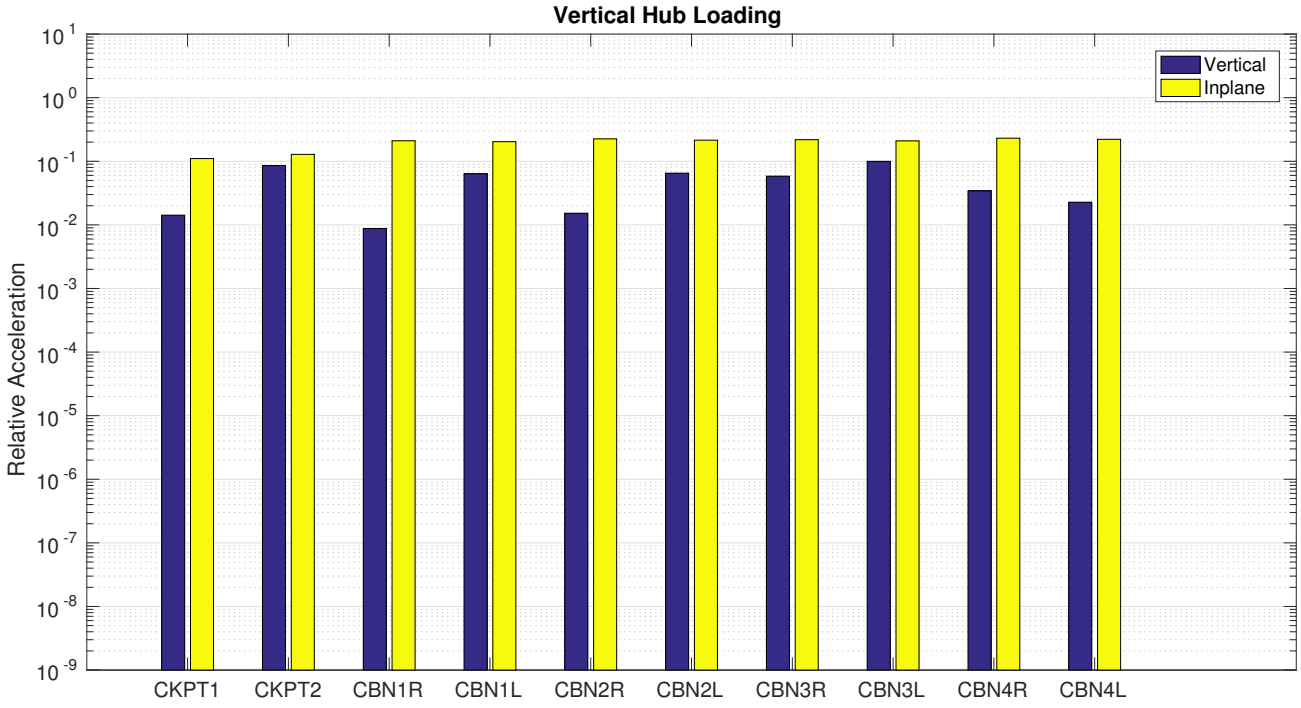

Figure 16: MVA+MSA: N_b/rev acceleration of two cockpit and eight cabin sensors due to vertical hub force, relative to the nominal plant in log scale.

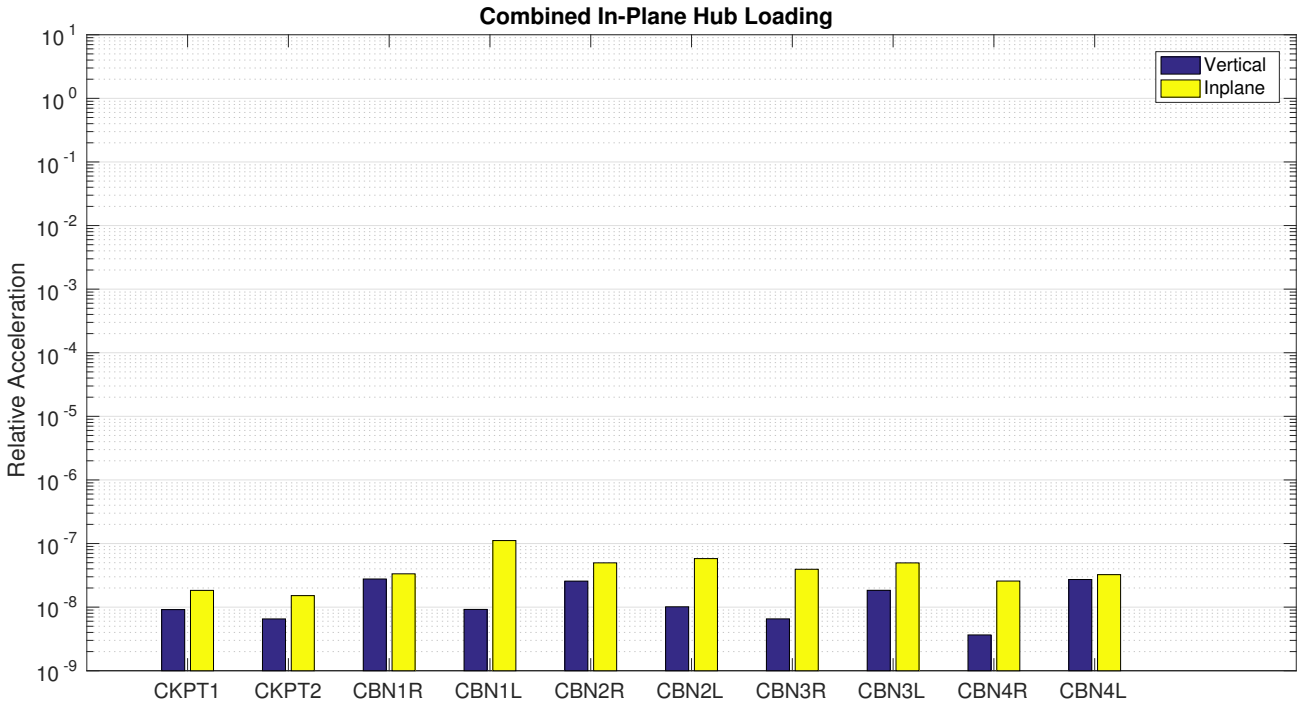

Figure 17: MVA+MSA: N_b/rev acceleration of two cockpit and eight cabin sensors due to combined in-plane hub force, relative to the nominal plant in log scale.

ACKNOWLEDGEMENTS

This work received partial support by Leonardo Helicopter Division. The authors particularly acknowledge LHD for providing the data used in the analysis.

References

[1] Pierangelo Masarati, Giuseppe Quaranta, Massimo Gennaretti, and Jacopo Serafini. An investigation of aeroelastic rotorcraft-pilot interaction. In *37th European Rotorcraft Forum*, Gallarate, Italy, September 13–15 2011. Paper no. 112.

[2] Giuseppe Quaranta, Aykut Tamer, Vincenzo Muscarello, Pierangelo Masarati, Massimo Gennaretti, Jacopo Serafini, and Marco Molica Colella. Rotorcraft aeroelastic stability using robust analysis. *CEAS Aeronaut. J.*, 5(1):29–39, March 2014. doi:10.1007/s13272-013-0082-z.

[3] Kristin L. Harrer, Debra Yniguez, Maria Majar Maria, David Ellenbecker, Nancy Estrada, and Mark Geiger. Whole body vibration exposure for MH-60s pilots. In *43th SAFE*, Utah, USA, 2005.

[4] A. R. S. Bramwell. *Helicopter Dynamics*. Edward Arnold, London, 1976.

[5] Rendy P. Cheng, Mark B. Tischler, and Roberto Celi. A high-order, linear time-invariant model for application to higher harmonic control and flight control system interaction. TR 04-005, NASA, 2006.

[6] Tomasz Krysinski and François Malburet. *Mechanical Vibrations*. ISTE Ltd, 2007.

[7] Richard L. Bielawa. *Rotary Wing Structural Dynamics and Aeroelasticity*. AIAA, Washington, DC, 2nd edition, 2005.

[8] R.A. Desjardins and W.E. Hooper. Rotor Isolation of the hingeless rotor BO-105 and YUH-61 helicopters. In *2nd European Rotorcraft and Powered Lift Aircraft Forum*, 1976.

[9] R.A. Desjardins and W.E. Hooper. Antiresonance rotor isolation for vibration reduction. In *American Helicopter Society 34th Annual Forum*, Washington DC, May 1978.

[10] D. Braun. Development of antiresonance force isolators for helicopter vibration reduction. In *6th European Rotorcraft Forum*, Bristol, UK, September 1980.

[11] P. Hege and G. Genoux. The SARIB vibration absorber. In *9th European Rotorcraft and Powered Lift Aircraft Forum*, September 1983.

[12] T. Krysinski, D. Ferullo, and A. Roure. Helicopter vibration control methodology and flight test validation of a self-adaptive anti-vibration system. In *24th European Rotorcraft Forum*, Marseille, FR, September 1998.

[13] D.R. Halmes. LIVE liquid inertia vibration eliminator. In *American Helicopter Society 36th Annual Forum*, Washington DC, May 1980.

[14] D.R. Halwes. Total main rotor isolation system. In *American Helicopter Society Northeast Region Specialist Meeting on Helicopter Vibration*, Hartford, CT, November 1981.

[15] D.R. Halwes. Total main rotor isolation system analysis. CR NAS1-16211, NASA, 1981.

[16] Dennis P. McGuire. Active vibration control using fluidlastic pylon struts. In *American Helicopter Society 62nd Annual Forum*, Phoenix, Arizona (USA), May 9–11 2006.

[17] M.N.H . Hamouda and G.A. Pierce. Helicopter vibration suppression using simple pendulum absorbers on the rotor blade. CR NSG-1592, NASA, 1982.

[18] R W White. A fixed frequency rotor head vibration absorber based upon G.F.R.P. springs. In *5th European Rotorcraft Forum*, Amsterdam, Netherlands, September 4–7 1979.

[19] J. T. Pearson, R. M. Goodall, and I. Lyndon. Active control of helicopter vibration. *Computing & Control Engineering Journal*, 5(6):277–284, December 1994. doi:10.1049/ccej:19940608.

[20] Norman D. Ham, Brigitte L. Behal, and McKillip Robert M., Jr. Helicopter rotor lag damping augmentation through individual-blade-control. *Vertica*, 7(4):361–371, 1983.

[21] N. D. Ham. Helicopter individual-blade-control research at MIT 1977–1985. *Vertica*, 11(1/2):109–122, 1987.

[22] Ch. Kessler. Active rotor control for helicopters: individual blade control and swashplateless rotor designs. *CEAS Aeronaut. J.*, available online, 2011. doi:10.1007/s13272-011-0001-0.

[23] C.R. Fuller, S.J. Elliott, and P.A. Nelson. *Active Control of Vibration*. Academic Press, 1996.

[24] Pierangelo Masarati, Vincenzo Muscarello, and Giuseppe Quaranta. Linearized aeroservoelastic analysis of rotary-wing aircraft. In *36th European Rotorcraft Forum*, pages 099.1–10, Paris, France, September 7–9 2010.

[25] Pierangelo Masarati, Vincenzo Muscarello, Giuseppe Quaranta, Alessandro Locatelli, Daniele Mangone, Luca Riviello, and Luca Viganò. An integrated environment for helicopter aeroservoelastic analysis: the ground resonance case. In *37th European Rotorcraft Forum*, pages 177.1–12, Gallarate, Italy, September 13–15 2011.

[26] Roy R. Craig, Jr. and Mervyn C. C. Bampton. Coupling of substructures for dynamic analysis. *AIAA Journal*, 6(7):1313–1319, July 1968.

[27] N.J. Mansfield. *Human Response to Vibration*. Taylor & Francis, 2004.

[28] Tobias Rath and Walter Fichter. A closer look at the impact of helicopter vibrations on ride quality. In *AHS 73rd Annual Forum*, Forth Worth, TA, USA, May 9–11 2017.

[29] Yong Chen, Upekha Senarath Yapa, Andrew Price, and Viresh Wickramasinghe. Evaluation of aircrew whole-body vibration and mitigation solutions for helicopter flight engineers. In *AHS 73rd Annual Forum*, Forth Worth, TA, USA, May 9–11 2017.

[30] Andrew H. Law, Heather E. Wright Beatty, Jocelyn Keillor, and Viresh Wickramasinghe. Pilot head and neck response to helicopter whole body vibration and head-supported mass. In *AHS 73rd Annual Forum*, Forth Worth, TA, USA, May 9–11 2017.

[31] Y. Wan and J. M. Schimmels. Optimal seat suspension design based on minimum simulated subjective response. *Journal of biomechanical engineering*, 119(4):409–416, 1997.